Fault Locator Using Travelling Waves: Experience in the Belgian Transmission Network

X. Bustamante-Mparsakis, J.C. Maun

***Abstract*— Travelling Waves (TWs) are electro-magnetic transients that are generated when there is a sudden change of voltage in the network, such as when a fault occurs. Fault locators based on TWs have recently emerged as an alternative to typical impedance fault locators thanks to their higher precision in most cases. The development of new algorithms based on TWs is improved by the understanding of their behaviors, in particular with the analysis of high frequency records of faults. Such records are not readily available. We performed a measurement campaign in the Belgian transmission network to acquire records of TWs generated when faults occur. This paper reports the experience acquired during the campaign, and discusses fault location algorithm improvements to account for the unique topology of the monitored line. The algorithm improvement reduces the error caused for non-homogeneous lines, which can be significant for big lines. The records analysis showed three important factors that influence the shape of the recorded TWs: the discontinuity in the line caused by a T-junction, the bandwidth of the measurement transformers, and the secondary cables connected to the current transformers. Therefore, those effects should be carefully considered when developing new algorithms based on TWs.**

***Keywords*: Fault location, Travelling waves, Field experience, Fault records.**

I. Introduction

After a fault occurs on the power network, the precise knowledge of the fault location is of significant importance, especially for long lines. It allows a fast dispatching on location to solve the problem.

When a fault occurs, the sudden change of voltage generates electro-magnetic transients: the Travelling Waves (TWs) [1], [2]. Those TWs propagate in both directions from the fault point, with a velocity close to the speed of light in overhead lines [1], [3]. The exact velocity depends on the geometry of the line.

The increasing performance of measurement devices made it possible to record TWs in substations. Travelling Wave Fault locators (TWFL) have thus recently emerged as an alternative to typical fault locators based on impedance measurements. They have a better precision, which is not affected by the fault resistance or load flow.

The most commonly used TWFL algorithm, the type-D [3], is based on measuring the arrival time of the first TW at both ends of the faulty line. For a good precision, the signals must be recorded with a high sampling frequency (typically higher than 1MHz), and a good time synchronization is needed between the records at both ends of the line.

While the classic type-D algorithm is simple, the attenuation and distortion of TWs make it difficult to precisely determine their arrival time. Due to their high velocity, an error of 1μs in the arrival time leads to an error of ~300m for the fault location. Many recent studies aim at developing algorithms that minimize this error [4]-[7].

It is dangerous to develop such algorithms based on simulations only, which represent a simplified version of reality due to the assumptions made. Many phenomena occurring when recording TWs are unexpected or otherwise difficult to model correctly. For example, the measurement transformers affect the high frequency signals. They are designed to perform at power frequencies, and few works have been done to study their bandwidth at high frequencies. Those studies agree that current transformers have a good bandwidth and provide a correct reproduction of current TWs, while voltage transformers have a poorer bandwidth and will significantly affect the voltage TWs recorded [3], [8]. The exact bandwidth of the measurement transformers is device-specific, and an accurate high frequency model of those transformers is a difficult task. Another effect seldom talked about is the secondary cable ringing, which significantly affects the signals recorded: fast reflections of TWs occur in the control cables connected to the secondary side of current transformers [4], [9].

The analysis of fault-induced transients recorded in actual substations is important to better the understanding of TWs, and to the development of fault location and protection algorithm based on TWs, and to the improvement of simulation tools. Such high-frequency fault records are not readily available and are difficult to acquire.

We performed a measurement campaign in the Belgian transmission network to acquire records of TWs generated when faults occur. We obtained time-synchronized records of one lightning-induced fault and of two line energizing.

This paper reports the experience acquired during the campaign, and discusses improvements to the classic type-D algorithm to account for the unique topology of the monitored line.

II. Measurement Campaign

We performed a measurement campaign to acquire records of TWs generated inside the power network when faults occur. The measurement devices were installed in substations on the Belgian transmission network to monitor a 70kV line.

X. Bustamante-Mparsakis and J.C. Maun are with the Department of bio, electro and mechanical systems, Free University of Brussel, Belgium. (e-mails: xbustama@ulb.ac.be, jcmaun@ulb.ac.be)

Paper submitted to the International Conference on Power Systems Transients (IPST2017) in Seoul, Republic of Korea June 26-29, 2017

A. Network Topology

The line that was monitored during the measurement campaign presents a unique topology (Fig. 1). A T-junction is present inside the line, but the additional branch is short (165m) and ends in a power transformer that was not connected to the network during the test period. Additionally, one section is a parallel line while the other section is a single line. Classical iron-cored current transformers and inductive voltage transformers were used to reduce the signals to be recorded. The currents are measured entering the line.

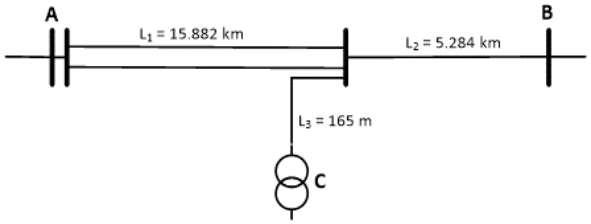

Fig. 1. Topology of the monitored 70 kV line. Measurements are performed in stations A and B.

Due to practical constraints on the trigger, different measurement equipment was used for recording faults and line energizing, and saturation is present in the energizing records. All the measurements are synchronized using GPS antenna with a precision of 100ns.

B. Records Overview

Six useful records were acquired: four fault records and two line-energizing records. Due to technical difficulties on the trigger, we only acquired time-synchronized records of one fault (Fig. 2). A succeeding similar fault record was acquired in substation A only. In addition, two line energizing records were acquired (Fig. 3). Those synchronized records will be developed in this paper. The power frequency was filtered out of all the records presented.

III. Propagation Speed

During the energizing of a line, the three phases are not closed simultaneously. Each phase closure generates new TWs. One energizing record can provide us with three propagation events to measure the propagation time. For our second record, only one phase closure is usable due to the voltage saturation of the records.

A. Propagation Time – Energizing Records

The propagation time was measured for each event (Table I). The total propagation time inside the monitored line is averaged as 72.125 µs, and is subject to errors caused by the time synchronization, the sag of the line and the error made when measuring it. This gives an average propagation speed inside the line of 293.46 m/µs.

The total propagation time is the sum of the propagation time inside the parallel line section and inside the single line section. The TW velocity inside each section is different due to the change in geometry. If we assume a constant speed in the line, an error is added to the fault location.

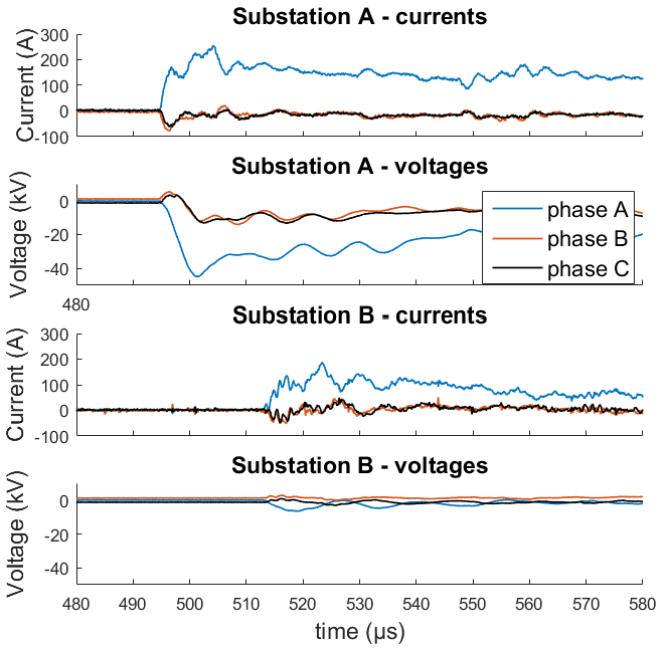

Fig. 2. Synchronized fault record during a lightning strike.

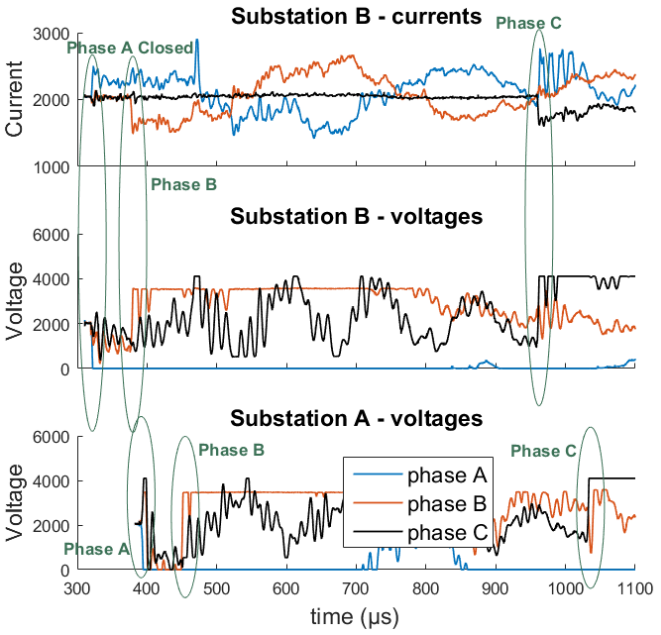

Fig. 3. Synchronized record during the re-energizing of the line.

TABLE I
PROPAGATION TIME MEASURED WITH THE ENERGIZING RECORDS

Phase closed	t_{prop} (µs)
A (event 1)	71.8
B (event 1)	72.3
C (event 1)	71.9
C (event 2)	72.5

B. Propagation Speed - Simulations

A typical overhead line was modelled in EMTP with a J-Marti line model, using the geometry of a specific line provided in [10]. The LCC routine of EMTP computes the line parameters (the distributed resistance, inductance, capacitance and conductance) based on its geometry. Single and parallel lines were modelled, and their geometry was varied. The line parameters are affected by this change in geometry, which modifies the propagation speed inside the line [11]. The propagation speed inside the lines for each modelled geometry is displayed in Table II. This analysis is just an example to illustrate the variability of the propagation speed, and real results will differ.

TABLE II
PROPAGATION SPEED INSIDE LINES MODELLED WITH EMTP

Parameter	Value	Propagation speed
Single line		
Conductor diameter	10 mm	298.5 m/μs
	20 mm	297.8 m/μs
	30 mm	297.4 m/μs
Phase distance	1 m	296.7 m/μs
	2 m	297.8 m/μs
	3.5 m	298 m/μs
Parallel line		
Lines distance	5 m	291.7 m/μs
	9 m	286 m/μs
	16 m	280.3 m/μs

The propagation speed in single lines has little variability with the changes in geometry. In parallel lines it is slower, and varies significantly with the distance between lines. The average propagation speed measured in the monitored line (293.46 m/μs) is in agreement with those results, since the line is composed of both single and parallel line sections.

C. Non-homogeneous Line Analysis

If we assume a constant speed in the line, an error is added to the fault location. It is impossible, in practice, to measure the propagation time in each section independently. Two options are available to account for the non-homogeneousness of the line:

- Model the lines in order to determine their parameters;
- Assume the velocity in one section of the line;

The first method consists in modelling the line to determine the propagation speed in each section. It requires the precise knowledge of the geometry of the line to determine the propagation speed based on the parameters.

We propose a solution where we assume the velocity inside the single line section. We make this assumption thanks to the small variability of propagation speed in single lines. The velocity inside the parallel section is then computed as in (2).

$$t_{prop} = t_{\sec 1} + t_{\sec 2} = \frac{L_1}{v_1} + \frac{L_2}{v_2} \tag{1}$$

$$v_1 = \frac{L_1}{t_{prop} - \frac{L_2}{v_2}} \tag{2}$$

Where t_{prop} is the total propagation time measured inside the line (s), t_{sec1} and t_{sec2} are the propagation time respectively in the parallel line section and in the single line section (s), v_1 and v_2 are the propagation speed in each section (m/s), L_1 and L_2 are the section lengths (m).

In this paper, we chose v_2=297.8 m/μs (based on [10]), which gives v_1=292 m/μs.

IV. FAULT LOCATION ALGORITHM

A. Classic Type-D Algorithm

The most frequently used TWFL algorithm is the so-called type-D [3]. The TWs generated at fault point propagate in both directions and reach stations A and B (Fig. 4). Such algorithms require measurements at both ends of a line with a good time synchronization, but have the advantage of requiring only the arrival time of the first TW. The fault location is computed as in (3).

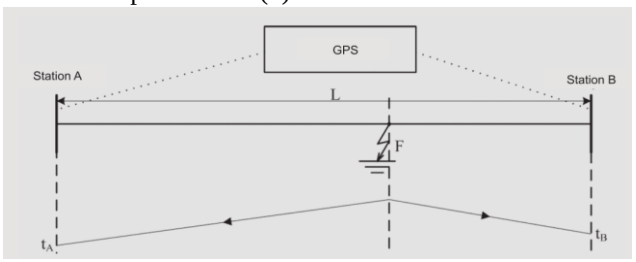

Fig. 4. Type-D fault locator [12].

$$D = \frac{L + v \cdot (t_A - t_B)}{2} \tag{3}$$

where D is the fault location from station A (m), v is the wave velocity (m/s), L is the line length (m), and t_A and t_B are the arrival times of the first incident wave at each station (s).

B. Type-D Algorithm for Non-Homogeneous Lines

Equation (3) is correct when the propagation speed is constant along the whole line. For non-homogeneous lines (such as the monitored line), the propagation speed differs depending on the section. The typical type-D algorithm has to be modified to account for this speed difference.

For a fault that occurs on section 1 of a line that consists of two distinct sections, the propagation times before reaching each station are expressed in (4) and (5). This leads to a fault location as expressed in (7).

$$t_A = \frac{D}{v_1} \tag{4}$$

$$t_B = \frac{L_2}{v_2} + \frac{L_1 - D}{v_1} \tag{5}$$

$$\Delta t = t_B - t_A = \frac{L_2}{v_2} + \frac{L_1 - D}{v_1} - \frac{D}{v_1} \tag{6}$$

$$D = \frac{L_1 - v_1 \cdot \Delta t}{2} + \frac{v_1 \cdot L_2}{2v_2} \quad (7)$$

Where t_A and t_B are the propagation time from fault point to stations A and B (s), D is the fault location (m), L_1 and L_2 are the lengths of each section (m), and v_1 and v_2 are the propagation speed in each section (m/s).

If the fault occurs on section 2, the fault location is found with (8). The use of this algorithm therefore requires a selection of which section is at fault. This can be done with the measurement of Δt and the knowledge of the topology.

$$D = L - \frac{L_2 - v_2 \cdot \Delta t}{2} - \frac{v_2 \cdot L_1}{2v_1} \quad (8)$$

Where L is the total length of the line (m).

C. Type-A Algorithm

Type-A fault location algorithms use the measurements on one side of the line only. The fault location is computed based on the measurement of the arrival time of the first TW, and the arrival time of the first reflection of that TW on the fault point, as depicted on Fig. 5.

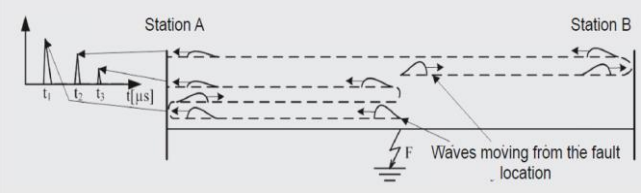

Fig. 5. Type-A fault locator [12].

$$D = \frac{t_3 - t_1}{2} \cdot v \quad (9)$$

Where t_1 is the arrival time of the first incident wave (s) and t_3 is the arrival time of the first reflection on fault point (s).

The main challenge in using type-A algorithms is to recognize the TW reflection on fault point from all the other reflections occurring in the network. In the example depicted in Fig. 5, the TW reflection on station B reaches station A (at t_2) before the desirable reflection on fault point (at t_3).

To avoid the need to identify each reflections, the arrival time of the first reflection can be approximated thanks to the fault location found with the type-D algorithm. The type-A algorithm can then be used as validation and correction. It removes a source of error coming from the time synchronization.

D. Application to Simulations

The typical and updated type-D algorithms were applied to a simulation model. The simulation models a non-homogeneous 50 km line with EMTP using the J-Marti line models described in section III. B. The first part of the line is a parallel line where the propagation speed is lower, and the second part is a single line (Fig. 6). The exact line models are not important to the discussion. The point of this section is to illustrate the importance to use an updated type-D algorithm for non-homogeneous lines where the velocity is not constant in the whole line. The fault occurs at 20km from station A.

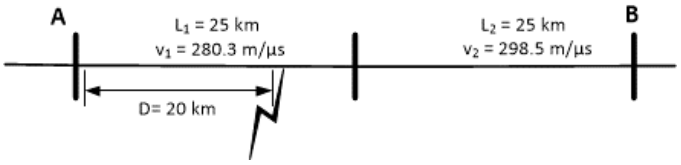

Fig. 6. Line modelled in EMTP

To illustrate the error introduced by each algorithm, the propagation speed inside each section is assumed unknown. The only available information is the measured total propagation time inside the line during energizing, and the measurement of Δt during the fault. Both algorithms are applied to find the fault location (Table III).

TABLE III
CLASSIC AND UPDATED TYPE-D ALGORITHMS APPLIED TO SIMPLE SIMULATIONS

Line data	
Section 1 velocity	280.3 m/μs
Section 2 velocity	298.5 m/μs
Measurements	
Total propagation time	172.94 μs
$\Delta t = t_B - t_A$	30.24 μs
Classic type-D computation	
Average speed	289.12 m/μs
Fault location	20.63 km
Updated type-D computation	
Section 2 speed (assumption)	297.8 m/μs
Section 2 speed (estimation)	280.93 m/μs
Fault location	20.04 km

When applying the classic type-D algorithm, the velocity inside the line is assumed homogeneous. This assumption introduces an error of 630m for this particular example.

The updated type-D algorithm assumes only the velocity inside the single line section. This assumption introduces a smaller error of 40m for the fault location.

E. Application to the Fault Record

The updated type-D algorithm was applied to our synchronized fault record, using the velocities previously computed. The fault location computed is inside the range provided by the TSO, and is validated by a type-A fault location algorithm (Table IV). A correction of 105m is applied with the type-A algorithm.

TABLE IV
TWFL ALGORITHMS APPLIED TO THE FAULT RECORD

TSO fault location	8.18 ± 1.63 km
Updated type-D	7.83 km
Expected 1st reflection	548.3 μs
Measured 1st reflection	547.6 μs
Type-A algorithm	7.725 km

V. Fault Records Analysis

We analyzed the fault records to understand and illustrate the different effects of the power network and substations on the TWs recorded.

A. T-Junction

Fast reflections are caused by the T-Junction. The T-Junction is a point of discontinuity in the system. At any point of discontinuity, reflections occur [1]. When the TW reach the T-Junction, part of the wave will continue through the line and part of the wave will be moving toward the power transformer in C (Fig. 1). Fast reflections ensue between the junction and the power transformer. This is only observable in the remote-end which has the T-Junction in-between it and the fault point (station B in our case).

The reflections should occur every 1.1 µs (eq. (10)) and are observed in Fig. 7.

$$T = \frac{2 \cdot L_3}{v_2} = 1.1\mu s \tag{10}$$

Where T is the time between two reflections caused by the T-Junction (s), L_3 is the length of the short line connected to the junction (m), and v_2 is the propagation speed inside the single line section (m/s).

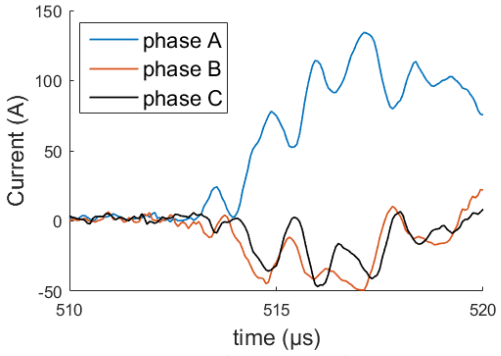

Fig. 7. The T-junction creates fast current reflections in substation B.

B. Voltage Transformers

It is agreed in the literature that voltage transformers have a worst bandwidth than current transformers [3], [8]. In our records, we found that in substation A, the voltage waves were clearly detectable, even if less steep than the current waves. In substation B however, the voltage waves are an order of magnitude lower with bigger reflections proportionally (Fig. 8).

This difference in voltages acquired and the frequencies that appear are not explained with the network and are believed to be heavily affected by the voltage transformers. The understanding of the voltage waves recorded will require additional work to be performed on the subject.

C. Current Transformers

Current transformers have a better bandwidth for TWs, but their secondary cables create ripples on the current waves [4], [9]. At one end of those secondary cables, the TW sees a high impedance (from the current transformer), and at the other end it sees a low impedance (the relay), which creates the fast reflections. The different cable lengths in each substation generates ripples of different period (Fig. 9).

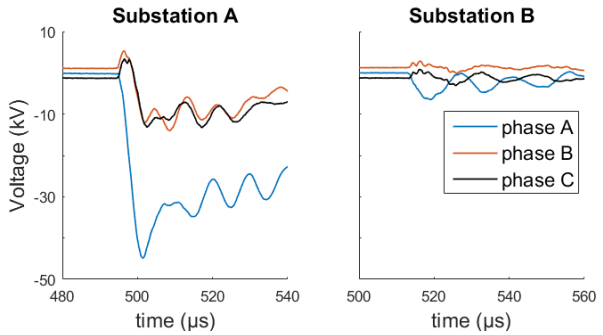

Fig. 8. The voltage waves in substation A are different from the voltage waves in substation B.

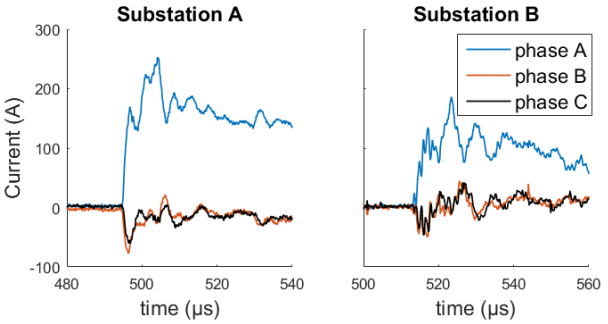

Fig. 9. The effect of current ripples caused by the CT secondary cabling is observed in both stations.

D. First Reflection on Fault Point

The expected arrival time of the 1st reflected TW in station A (t=548.3 µs) was computed on section *IV E*. This reflection is not observable in station B due to the T-Junction, creating too many pre-reflections before the reflection on fault point.

In station A, this reflection can be detected better with the currents than with the voltages (Fig. 10). It is challenging to recognize this first reflection from all the other events occurring with the TWs, but the arrival time of the first reflection was successfully used as a validation of the type-D algorithm.

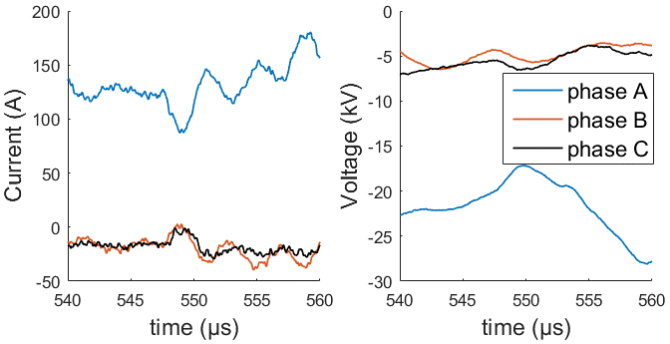

Fig. 10. The first reflection should occur at t=548.3µs based on the computed fault location.

E. Successive events

Successive records for distinct lightning strokes provide similar shapes (Fig. 11), which show that the results are reproducible for different but close lightning strokes (1.4 km apart in this case) and must be explained by the network and the substations. Data from the phase C fault have been inverted in order to better compare the results.

In those records, we observe that the current and voltage waves display similar shapes. This is expected, since the TWs are reduced with the same measurement transformers.

The current ripples caused by the CT secondary cables have the same reflection period, but with different amplitude. The period depends on the length of the secondary cables and is constant for a given substation. The amplitude depends on the fault location (a further fault will delay the arrival of ground mode waves) and on the incident wave amplitude.

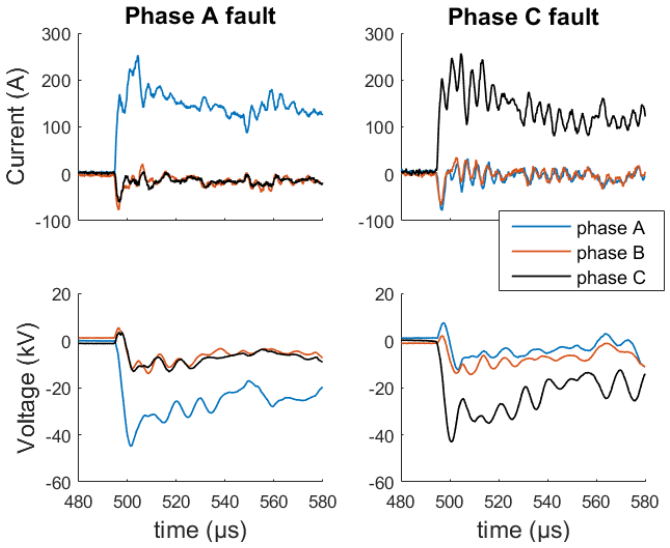

Fig. 11. The signals in substation A are similar for similar events (lightning strokes ~1.4 km apart).

F. Waves polarity

The polarity of the waves are in coherence with the analysis found in the literature. In [13], we see that for faults occurring on the line, the TW from one phase has a different polarity from the other two. In [14], we see that the current and voltage waves measured in one substation have a different polarity for forward faults.

VI. Conclusions

This paper presented an update of the classic type-D fault location algorithm. This updated algorithm takes into account non-homogeneous lines. It was applied to EMTP simulations and field records, and was validated with a type-A algorithm. It decreases the error caused by non-homogeneous line when using a type-D TWFL.

This paper also presented fault records of TWs generated during a fault, and during the energizing of a line in the Belgian transmission network. The analysis of the records showed that three factors significantly affect the shapes of recorded TWs: the discontinuities inside the line, the bandwidth of the measurement transformers, and the secondary cables connected to the current transformers.

Those effects are difficult to model, and should be carefully considered when developing new algorithms based on TWs. The records presented in this paper can be used to improve and validate simulation models for high frequencies suitable for TWs studies.

VII. Acknowledgment

The authors gratefully acknowledge Elia, the Belgian transmission system operator, for the opportunity to perform a long-term measurement campaign in their substations.

VIII. References

[1] L. Van der Sluis, Transients in Power Systems. Chichester: John Wiley & Sons Ltd, 2001.

[2] A. M. Elhaffar, “Power transmission line fault location based on current traveling waves,” Ph.D. dissertation, Dept. of Elec. Eng., Univ. of technology, Helsinki, 2008.

[3] G. Krzysztof, R. Kowalik, D. Rasolomampionona, and S. Anwar, “Traveling wave fault location in power transmission systems: an overview,” *J. Electr. Syst.*, vol. 3, no. 7, pp. 287–296, 2011.

[4] S. Marx, B. K. Johnson, A. Guzmán, V. Skendzic, and M. V Mynam, “Traveling Wave Fault Location in Protective Relays : Design , Testing , and Results,” in *16th Annual Georgia Tech Fault and Disturbance Analysis Conference*, 2013, pp. 1–14.

[5] G. Krzysztof and D. D. Rasolomampionona, “Travelling wave fault location algorithm in HV lines - Simulation test results for arc and high impedance faults,” in *IEEE EuroCon 2013*, 2013, no. July, pp. 724–730.

[6] G. Zhang, H. Shu, and Y. Liao, “Automated double-ended traveling wave record correlation for transmission line disturbance analysis,” *Electr. Power Syst. Res.*, vol. 136, pp. 242–250, 2016.

[7] F. V Lopes, S. Member, and W. L. A. Neves, “Fault Location on Transmission Lines Based on Travelling Waves,” in *International Conference on Power systems Transients*, 2011.

[8] M. A. Redfern, S. C. Terry, F. V. P. Robinson, and Z. Q. Bo, “A Laboratory Investigation into the use of MV Current Transformers for Transient Based Protection,” in *International Conference on Power systems Transients*, 2003.

[9] D. J. Spoor, J. Zhu, and P. Nichols, “Filtering effects of substation secondary circuits on power system traveling wave transients,” in *2005 International Conference on Electrical Machines and Systems*, 2005, p. 2360–2365 Vol. 3.

[10] W. Dommel, “Overhead transmission lines," in *EMTP theory book*. Vancouver, British Columbia. 1981, pp. 4-1 – 4-107,

[11] Working group D6, “AC Transmission Line Model Parameter Validation,” for the IEEE Power & Energy Society, Sept. 2014.

[12] G. Krzysztof, R. Kowalik, and D. Rasolomampionona, “Travelling wave fault location in hv lines.”

[13] Y. Liu, G. Sheng, Y. Hu, X. Jiang, Y. Sun, and S. Wang, “Identification of back flash and shielding failure on transmission line based on time domain characteristics of traveling wave,” in *IEEE Power and Energy Society General Meeting*, 2014.

[14] E. O. Schweitzer, B. Kasztenny, A. Guzmán, V. Skendzic, M. V Mynam, and S. E. Laboratories, “Speed of Line Protection – Can We Break Free of Phasor Limitations ?,” in *68th Annual Conference for Protective Relay Engineers*, 2015, pp. 448–461.